

A Plasma-Based Approach for High-Power Tunable Microwave Varactors

Samsud Moon
mmoon4@rockets.utoledo.edu

Abstract—This work presents a tunable varactor with tunability in the range of 100s of MHz and a capacitance delta of about 36 pF by employing a perpendicular magnetic field to a capacitively-coupled (CCP) RF plasma cell. A comprehensive high-frequency circuit model for the fabricated varactor is proposed and verified experimentally for a plasma electron number density of $2.95 \times 10^{17} m^{-3}$ which has a tunability of 146 MHz with a magnetic flux density ranging from 0 to 246 milliTesla. Under a pressure of 64 milliTorrs, the Argon ccp was found to have a variable capacitance ranging from 4 pF to 41.72 pF.

Index Terms—Varactor, plasma, magnetic field, tunability

I. INTRODUCTION

As the demand for re-configurable RF systems increases, use of varactors becomes trivial due to their variable impedance. Front-end microwave and RF components such as voltage-controlled oscillators (VCOs), phase-shifters and phase-locked loops (PLL) depend on varactor tuning, their Q-factor and peak capacitance at certain frequencies at the RF/microwave range. Decades of improvement in semiconductor technology has made solid-state varactors the most widely used type in this domain of tunable RF devices. Film-based varactors have been previously reported [1], [2] to improve the Q-factor over the MOS [4]–[6] and MSM [3] based varactors that suffer from low Q and inability to withstand high power microwaves (HPM).

Plasma has been an element of interest lately because of its unique attribute of providing negative capacitance and tunability over a wide range of RF/microwave frequencies. Several works [8], [10], [15] previously reported the use of plasma as an impedance-matching entity for electrically small antennas. This work aims to exploit the plasma properties further by introducing a magnetic field perpendicular to the applied electric field and in turn enhancing varactor tunability as well as the capacitance ratio.

II. THEORY AND DESIGN OF PLASMA VARACTOR

For convenient numerical analysis, CCPs can be modeled having a relative permittivity, ϵ_{rp} and electrical conductivity, σ_p with an electron number density n_e by the expressions [12],

$$\epsilon_{rp} = 1 - \frac{e^2 n_e}{\epsilon_0 m (\omega^2 + v_m^2)}, \quad (1)$$

$$\sigma_p = \frac{e^2 n_e v_m}{m (\omega^2 + v_m^2)}, \quad (2)$$

where v_m is the electron-neutral collision frequency and ω is the EM frequency. A change either in electron density or

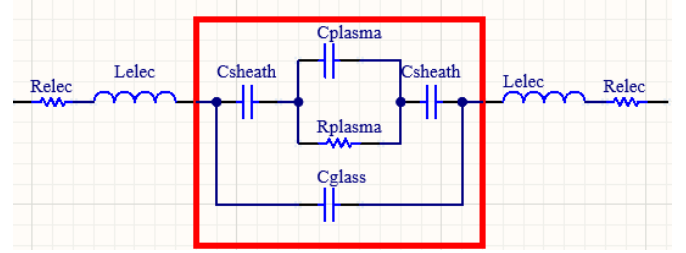


Fig. 1. Lumped circuit model for capacitively-coupled plasma with metal electrodes.

collision frequency will yield a variance in the permittivity and conductivity of the plasma cell. Insertion of a magnetic field normal to the propagation will alter the electron number density profile which was reported by [13] and [14]. The proposed device shown in Figure 2 is fabricated on a Rogers TMM10i substrate housing a plasma cell with an inner radius of 15 mm and a glass tube thickness of 1 mm. The design was chosen to minimize the loss of electrons and ions due to collision to the walls as well as to enable gas breakdown at a significantly low electric field. As the plasma excitation signal will have high power, the larger dimension was chosen to be around 0.1λ of the maximum frequency to diminish any radiation losses. To maintain electron confinement without significantly reducing the electron density, a permanent magnet of cylindrical shape with a diameter of 6 mm having a maximum magnetic flux density of 0.246 T was chosen. It is convenient to portray the capacitively-coupled plasma cell in a combination of circuit components, as it reduces the computational burden. A lumped model for commercially available gas discharge tubes was previously presented in [9]. With very subtle approximation, the topology can be modified to have a simplified circuit model without losing any significant accuracy. The modified model is depicted in Fig-1.

The fabricated device exhibits behaviors of a cylindrical capacitor with vacuum as the dielectric material in the absence of plasma.

When the gas is ignited, the parameters can be modeled as,

$$R_{plasma} = \frac{d - 2d_{sh}}{\sigma_p A_p}, \quad (3)$$

$$C_{plasma} = \frac{\epsilon_0 \epsilon_{rp} A_p}{d - 2d_{sh}}, \quad (4)$$

$$C_{sheath} = \frac{\epsilon_0 A_p}{d_{sh}}, \quad (5)$$

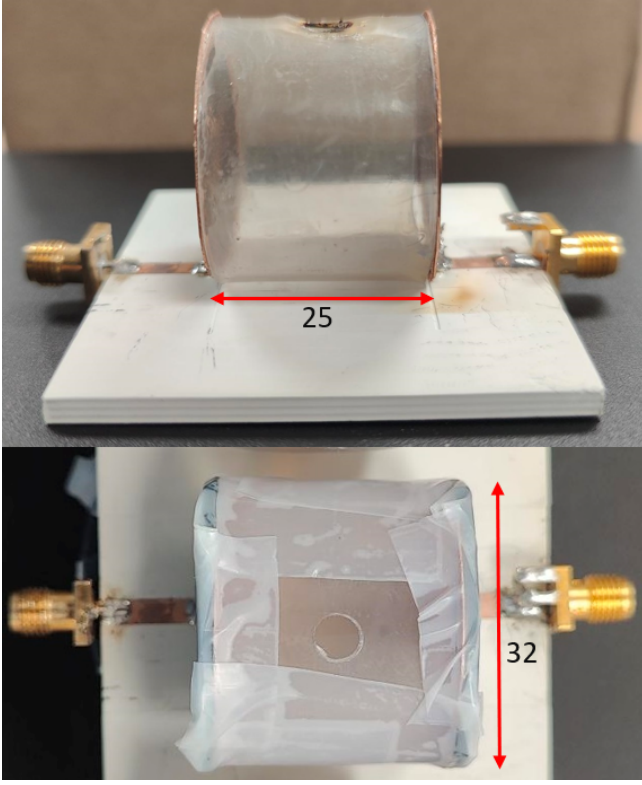


Fig. 2. Fabricated device on TMM10i substrate. The dimensions are in mm.

$$C_{glass} = \frac{\epsilon_0 \epsilon_g A_{glass}}{d}, \quad (6)$$

where d_{sh} is the sheath thickness near the electrodes, d is the gap between the powered electrodes, A_p and A_{glass} are the plasma area and the total area filled by the glass tube respectively. Aided by these parameters, a comprehensive numerical analysis is carried out by commercially available software like Keysight Advanced Design System(ADS). The simulation results paired with the experimental verification are presented in the next section.

III. MEASUREMENT AND RESULTS

The fabricated device was tested inside a vacuum chamber filled with Argon at 64 millitorr pressure. The magnet was attached to the head of a linear actuator which was controlled by a 12V DC power source, as depicted in Fig. 3a. At the starting position, the magnet was kept farthest position possible with a measured magnetic flux intensity of 0 T at the closest boundary of the device from the magnet. Afterwards, the input power was gradually increased with an excitation frequency of 100 MHz. The plasma ignited at 19.83 W of input power and was then reduced to 4.28 W to sustain the discharge at the region between the electrodes, as the Fig. 3b shows. The scattering parameters were then analyzed with a Fieldfox handheld microwave analyzer from a frequency range of 200 MHz to 1 GHz with a low power coupled probing signal. Once the plasma was stable, the magnet was then gradually brought

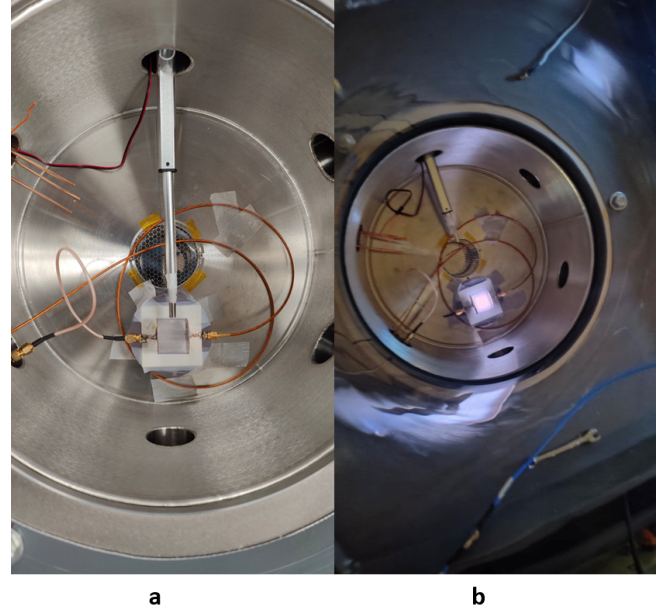


Fig. 3. a) Linear actuator with a permanent magnet attached to it's pole, b) Ignited argon plasma at B=0 T.

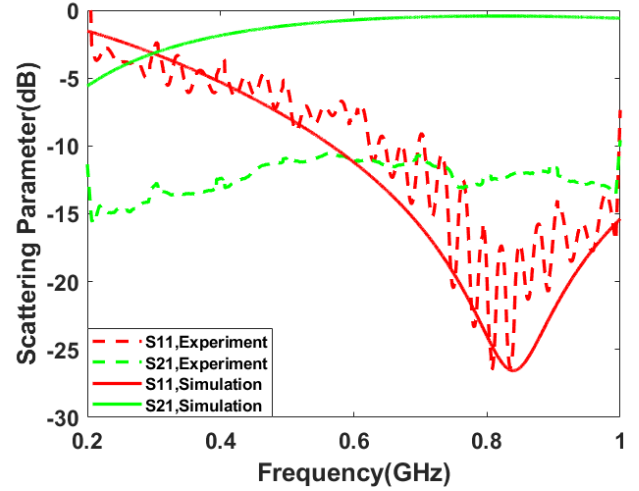


Fig. 4. Comparison of plasma scattering parameters for simulation and experimental results in the presence of magnetic field.

to the device's dielectric wall at the center position between the two electrodes by changing the voltage polarity of the actuator. The magnetic flux density was measured to be 0.246 T at this position. The scattering parameters were recorded in the presence of magnetic field. The derived electron density without any magnetic field was found to be $2.95 \times 10^{17} m^{-3}$ from the optimized circuit model in Figure 1.

In Fig. 4 the reflection and transmission coefficients of the fabricated device are compared for both simulated and experimental cases. The reflection for both cases are under significant agreement between the values. On the contrary, the Argon plasma under experiment has an offset of about -10dB for transmission coefficient over the whole frequency range for

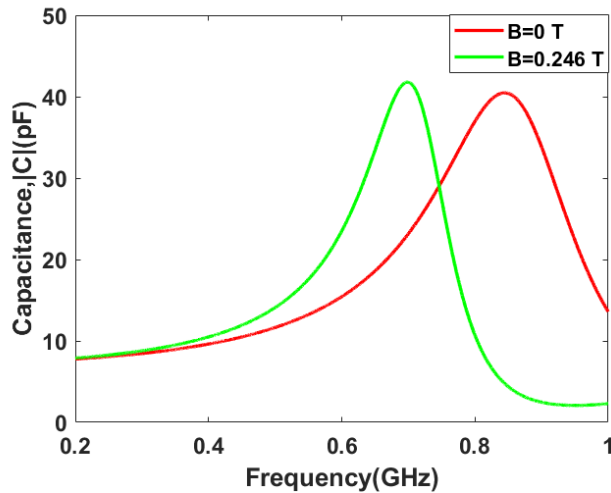


Fig. 5. Shift in the peak capacitance due to imposed magnetic field.

the measured scenario due to plasma being a lossy dielectric with collisional, thermal and electric losses. The dynamics in the value of capacitance are also observed in Fig. 5 as the peak value shows a frequency shift of 146 MHz and the $C_{max} - C_{min}$ reaches 36pF with a max/min ratio of 10.39:1. This device was tested to have absorbed up to 47.8 dBm of 100 MHz signal until the capacity of the power amplifier was peaked.

IV. CONCLUSION

A magnetically tuned plasma varactor with high tuning ratio and variable capacitance for a wide range of frequency is demonstrated as proof of concept. The inherently capacitive fabricated device is capable of producing a maximum capacitance of 41.72 pF in magnitude with the presence of a magnetic field with magnetic flux density of 246 milliTesla. The theory and simulations are then verified with experimental data. The tuning capability can further be improvised by varying plasma parameters as well as the magnetic field intensity and the size of magnets. Owing to isolation difficulties between the high powered excitation signal and probing signal during the measurement, the sinusoidal ripples in the measured data was prominent. Despite this, the proposed device can be very useful for certain applications where varactors capable of withstanding extreme high power microwaves are necessary.

V. ACKNOWLEDGMENT

This research was supported by the Applied Radio-frequency and Plasma Lab (ARPL) of The University of Toledo.

REFERENCES

[1] K. Annam, D. Spatz, E. Shin and G. Subramanyam, "Experimental Verification of Microwave Phase Shifters Using Barium Strontium Titanate (BST) Varactors," 2019 IEEE National Aerospace and Electronics Conference (NAECON), Dayton, OH, USA, 2019, pp. 63-66, doi: 10.1109/NAECON46414.2019.9058107.

[2] A. Tumarkin et al., "Ferroelectric Varactor on Diamond for Elevated Power Microwave Applications," in IEEE Electron Device Letters, vol. 37, no. 6, pp. 762-765, June 2016, doi: 10.1109/LED.2016.2554882.

[3] Chun San Chu, Yugang Zhou, K. J. Chen and K. M. Lau, "Q-factor characterization of RF GaN-based metal-semiconductor-metal planar interdigitated varactor," in IEEE Electron Device Letters, vol. 26, no. 7, pp. 432-434, July 2005, doi: 10.1109/LED.2005.851181.

[4] S. P. Bruss and R. R. Spencer, "A Continuously Tuned Varactor Array," in IEEE Microwave and Wireless Components Letters, vol. 19, no. 9, pp. 596-598, Sept. 2009, doi: 10.1109/LMWC.2009.2027096.

[5] Y. Oh, S. Kim, S. Lee and J. -S. Rieh, "The Island-Gate Varactor—A High-Q MOS Varactor for Millimeter-Wave Applications," in IEEE Microwave and Wireless Components Letters, vol. 19, no. 4, pp. 215-217, April 2009, doi: 10.1109/LMWC.2009.2015499.

[6] T. Quemerais, D. Gloria, D. Golanski and S. Bouvot, "High-Q MOS Varactors for Millimeter-Wave Applications in CMOS 28-nm FDSOI," in IEEE Electron Device Letters, vol. 36, no. 2, pp. 87-89, Feb. 2015, doi: 10.1109/LED.2014.2378313.

[7] J. S. Pulskamp, S. S. Bedair, R. G. Polcawich, C. D. Meyer, I. Kierzewski and B. Maack, "High-Q and Capacitance Ratio Multi-layer Metal-on-Piezoelectric RF MEMS Varactors," in IEEE Electron Device Letters, vol. 35, no. 8, pp. 871-873, Aug. 2014, doi: 10.1109/LED.2014.2327611.

[8] Abbas Semnani, Kushagra Singhal, Samsud Moon, "Impedance Matching in Small Antennas through Capacitively-Coupled Plasma Technique," 76th Annual Gaseous Electronics Conference Monday–Friday, October 9–13, 2023; Michigan League, Ann Arbor, Michigan

[9] S. N. Ramesh, and A. Semnani, "A Comprehensive Circuit Modeling Approach for Self-Sustained Capacitively Coupled Microwave Plasmas", *IEEE Transactions on Plasma Science*, vol. 49, no. 9, pp. 2690 - 2699, Sept. 2021.

[10] A. Semnani, K. Singhal and S. T. Moon, "A Plasma-Based Technique for Wideband Matching of Electrically Small Antennas," 2023 IEEE International Symposium on Antennas and Propagation and USNC-URSI Radio Science Meeting (USNC-URSI), Portland, OR, USA, 2023, pp. 1349-1350, doi: 10.1109/USNC-URSI52151.2023.10237701.

[11] A. Semnani, D. Peroulis and S. O. Macheret, "Plasma-Enabled Tuning of a Resonant RF Circuit," in IEEE Transactions on Plasma Science, vol. 44, no. 8, pp. 1396-1404, Aug. 2016, doi: 10.1109/TPS.2016.2588480.

[12] Y. P. Raizer, Gas Discharge Physics, Berlin: Springer-Verlag, 1991.

[13] Kim, M. K. (2009). Electromagnetic Manipulation of Plasma Layer for Re-Entry Blackout Mitigation (Doctoral dissertation).

[14] M. S. T. Moon, 'Effects of Magnetic Fields on the Electromagnetic Properties of Capacitively-Coupled Plasma', The University of Toledo, 2023.

[15] A. Semnani, K. Singhal and S. T. Moon, "A Plasma Matching Approach to Realize Wideband and Efficient Small Antennas," 2023 IEEE International Conference on Plasma Science (ICOPS), Santa Fe, NM, USA, 2023, pp. 1-1, doi: 10.1109/ICOPS45740.2023.10481261.